

Department of Electrical  
and  
Computer Systems Engineering

Technical Report  
MECSE-14-2005

An Optical Fiber Dispersion Measurement Technique and  
System

LN Binh and Itzhak Shraga

**MONASH**  
**UNIVERSITY**

# **An Optical Fiber Dispersion Measurement Technique and System**

Le Nguyen Binh and Itzhak Shraga<sup>1</sup>

Department of Electrical & Computer Systems Engineering, Monash University,  
Clayton Campus, Victoria 3168, AUSTRALIA

## **Abstract**

*We present a method of measurement of dispersion of guided optical medium, the optical fibre using microwave photonic techniques. Experimental set-up and theoretical development of the measurement systems are described. Analytical results are compared with those obtained experimentally for a length of 19.8 km standard single mode fibre.*

---

<sup>1</sup> On leave from Israel. The experimental work was conducted in 2003.

## Table of Contents

1	Introduction.....	3
2	The external modulation and dispersion .....	4
2.1	The Mach-Zehnder modulator .....	4
2.2	The dispersion parameter measurement.....	9
3.	Experimental Setup and Results .....	12
3.1	Experimental Setup.....	12
3.2	Measurement of the Mach-Zehnder Modulator Transfer Function .....	14
3.3	Measurement of Dispersion Parameter .....	16
	REFERENCES .....	19
	Appendix B. – Thermistor’s Coefficients calculation for Fujitsu FLD150F1CJ Laser .....	21
	Appendix C: Measurement results for one SM fiber spool (19.8km) and two fiber spools (39.6km).....	22

### List of Figures

<i>Figure 1 Typical electrode configuration for a waveguide phase modulator on insulating crystals as LiNbO<sub>3</sub> (a) single electrode driven modulator structure with On and OFF states (b) dual electrode type. ....</i>	<i>5</i>
<i>Figure 2 – Typical behavior of <math>\Delta P</math> as a function of <math>\psi_{k_m}^2</math> for <math>\alpha=1</math>.....</i>	<i>12</i>
<i>Figure 3 – Schematic diagram of the experimental setup.....</i>	<i>14</i>
<i>Figure 4 Measured transmission function and theoretical <math>\cos^2</math> fit.....</i>	<i>16</i>
<i>Figure 5 – Experimental results (error bars) and calculated results for fiber spool length <math>L_F=19.8km</math>.....</i>	<i>18</i>
<i>Figure 6 – Experimental results (error bars) and calculated results for fiber spool length <math>L_F=39.6km</math>.....</i>	<i>19</i>

### List of Tables

<i>Table 1 – Measured parameters.....</i>	<i>15</i>
<i>Table 2. – Experimental results with one 19.8km SM fiber spool.....</i>	<i>22</i>

## 1 Introduction

Modern optical communication systems demand higher and higher bandwidth and bit-rates. The state of the art Communication systems use already bit-rates of up to 40 Gbit/sec per channel and DWDM systems with up to 176 channels working at this bit-rate have been demonstrated [1]. Commercial optical communication systems use the already installed fiber-optic cables including standard Single Mode Fibers (SSMF) and 1.55 $\mu$ m Distributed Feedback (DFB) Lasers, available with multiple wavelengths at 0.8nm spacing (100GHz) or much narrower. Usually, the optical carrier is modulated by the electrical signal using one of the two most common modulation techniques: direct modulation of the DFB laser or use of an external modulator.

Direct modulation of the laser is the simplest approach. However when the laser must be biased close to the threshold current point and the digital signal is superimposed in order to switch the laser optical output on and off for the "1" and the "0" digital states. This approach introduces three separate limitations on the bit-rate: frequency chirp of the optical carrier, relaxation oscillations of the laser optical output power and bandwidth limitation due to parasitic inductance and capacitance of the laser packaging [2]. The relaxation oscillations of the laser and packaging parasitic inductance and capacitance limit the practical modulation frequency to 10GHz maximum, although, special designs allowed modulation frequencies up to 25GHz to be achieved. The frequency chirp limits the performance of the optical communication systems by reducing the "effective bandwidth" of the fiber (or by causing a pulse broadening), especially when 1.55 $\mu$ m laser is used in conjunction with standard SM fibers. In these systems, the bit-rate\*distance is limited to about 200Gbit\*km/sec [2].

Long-haul transmission of high bit-rates optical signals is mostly based on external modulation technique. The DFB laser is biased at a well-controlled DC bias and temperature, producing a very stable optical power output, both in amplitude and wavelength. The laser's optical output is passed through a separate device that modulates the optical carrier intensity – the external modulator. In this way, the unwanted effects of the direct modulation of the laser are avoided and the quality of the optical signal transmitted enables long-haul transmission over standard SM fibers. The only limitations of the system's bit-rate are imposed then by the attenuation and

dispersion of the fiber, since the standard SM fibers have significant dispersion parameter ( $\sim 18\text{ps/nm}\cdot\text{km}$ ) at the  $1.55\mu\text{m}$  laser wavelength. Compensation of the dispersion (using additional “negative dispersion” fibers) and calculation of the achievable bit-rate of optical communication systems require an accurate measurement of the fiber’s dispersion parameter.

There are few types of external modulators described in the literature [3],[5]: loss modulator, directional coupler modulator, total internal reflection modulator and Mach-Zehnder modulator, the last one being one of the most popular external modulators used. This report summarizes the theoretical background, description and results of an experiment conducted in the Optical Communications and Applied Photonics Laboratory. In this experiment we try to evaluate the dispersion parameter of a standard SM fiber using an externally modulated DFB laser with  $\lambda=1.55\mu\text{m}$  by a  $\text{LiNbO}_3$  Mach-Zehnder external modulator.

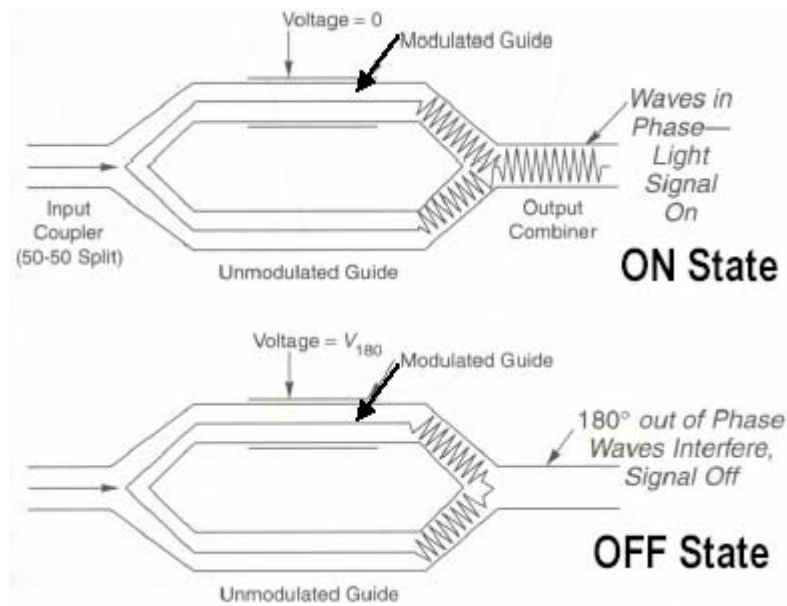
## 2 The external modulation and dispersion

This section presents some background information and theoretical approaches regarding the Mach-Zehnder interferometric modulator behaviour and the optical fiber dispersion parameter measurement technique.

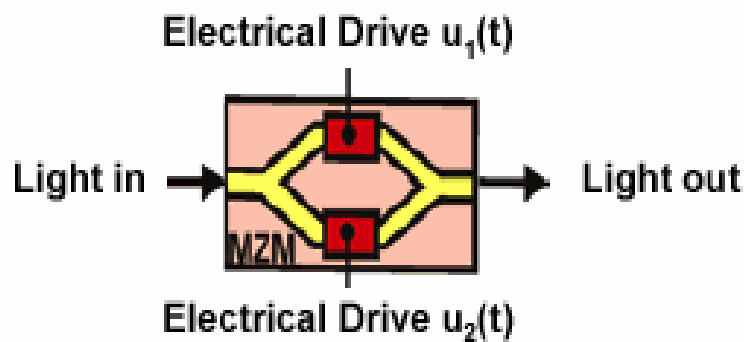
### 2.1 The Mach-Zehnder modulator

The Mach-Zehnder interferometric modulator has been extensively investigated and reported in the literature since 1980’s as a potential electro-optic modulator for high digital bit-rate and RF transmission over optical fiber communication systems [3]-[7]. There are different types of intensity modulators described in the literature based on the linear electro-optic (Pockel) effect, which provides a change in the optical waveguide refractive index proportional to the applied electric field. As a result, a phase change occurs for the incident optical field polarized in the direction of the electrical applied field.

One of the materials mostly used for electro-optic modulators is the  $\text{LiNbO}_3$  crystal with Ti:diffused waveguides. A waveguide phase modulator appropriate to Ti: $\text{LiNbO}_3$  is shown in **Figure 1**.



(a)



(b)

Figure 1 Typical electrode configuration for a waveguide phase modulator on insulating crystals as  $\text{LiNbO}_3$  (a) single electrode driven modulator structure with On and OFF states (b) dual electrode type.

The configuration of **Figure 1(a)** is used to induce a phase change in a TE mode for X-cut Y propagating (or Y-cut X propagating) crystals while **Figure 1(b)** shows the electrode configuration for a Z-cut orientation providing maximum phase change for the TM mode. The modulator used in this work is based on a Z-cut  $\text{Ti:LiNbO}_3$  crystal (see appendix A, for detailed data sheet), with a coplanar wave-guide structure (CPS).

The way in which the phase change of the optical field transforms in intensity modulation depends upon the device geometrical configuration and one of these configurations is the Mach-Zehnder interferometer. The modulator shown in **Figure 1b** is of an early design, in which both arms were driven by opposite polarity voltage

signals. Although this approach has some theoretical advantage by achieving a better optical signal quality (zero frequency chirp [5]), at very high frequencies, it is very difficult to match the impedance of the electrode to the RF source, for a broadband frequency range. Most of the high frequency modulators are implemented with only one traveling wave-guide electrode, as shown in 2b, exciting one arm of the modulator, as is the one used in this work. This electrode is matched to and terminated with the same characteristic impedance as the signal source (typically 50Ω) so no standing waves are formed along the interaction region. In this way, a very broadband device can be built [6]. There are some modulators on the market with two symmetrical traveling wave electrodes, allowing achieving zero chirp or other modulation schemes (like Single Side Band) with a very large bandwidth at high frequencies [10].

The physics of operation has been extensively discussed in the literature [3], [5] and will only be briefly reviewed here. The guided-wave interferometer shown in **Figure 1** modulates the light intensity due to the phase difference that is electro-optically induced between the two arms (in the traveling wave-guide electrode configuration, the phase shift is electro-optically affected in one arm only). The input power  $I_o$  is divided in two halves at the input Y branch (which acts as a 3dB splitter) and travel along the two arms, having (usually) the same physical and optical length. At the output Y branch the optical fields recombine. If the guided modes are in-phase, they will constructively interfere and excite the lowest order mode of the output wave-guide. If they are exactly 180° out of phase, then they recombine to excite the first antisymmetric mode, which is cut off and rapidly attenuated. Since the phase shift in the modulator's arms is affected only for the optical field polarized in the same direction as the exciting electrical field, the Mach-Zehnder modulator is very sensitive to the polarization of the input optical field and, usually, a very stable polarized optical source is required and a Polarization Maintaining Fiber (PMF) should be used between the source and the modulator input port.

Assuming an ideal device (no insertion loss), the optical field at the interferometer output is given by [4]:

$$E_O = \frac{E_I}{2} e^{(j\beta_1 L)} + \frac{E_I}{2} e^{(j\beta_2 L)} = E_I \cos(\Delta\beta L) e^{(j\bar{\beta} L)} \quad (1)$$

where  $E_O$  is the output optical field,  $E_I$  is the input optical field,  $\beta_1$  and  $\beta_2$  are the propagation constants in arm 1 and 2 of the interferometer,  $L$  is the arm's length and

$$\Delta\beta = (\beta_1 - \beta_2)/2 \quad (2)$$

$$\bar{\beta} = (\beta_1 + \beta_2)/2 \quad (3)$$

The cosine term in (1) provides the amplitude modulation while the exponential term produces the time dependent phase variation, or chirp. It can be seen from (1) that the phase modulation can be completely compensated if the propagation constants of the two wave-guides (arms) are changing by the same amount and with opposite signs, using two exciting voltage signals with equal amplitude and opposite polarity. In this way one can achieve (theoretically) a zero-chirp modulator.

The output intensity of the light as a function of the input intensity is given by [6], [7]:

$$\frac{I_O}{I_I} = \frac{|E_O|^2}{|E_I|^2} = A \cos^2(\Delta\beta L) = A \cos^2\left(\frac{\pi V_M}{2V_\pi}\right) \quad (4)$$

where  $A$  is the optical insertion loss of a practical device and  $V_M$  is the modulating signal voltage.  $V_\pi$  is the voltage required to change the output light intensity  $I_O$  from its maximum value to its minimum value and this parameter is related to the interferometer constants as follows:

$$V_\pi = K \frac{\lambda}{L} \quad (5)$$

where  $\lambda$  is the optical wave-length (in vacuum) and  $K$  is a constant related to geometrical and crystal parameters. It is important to point out that  $V_\pi$  and the phase shift is wave-length dependent so the Mach-Zehnder interferometer acts as an optical filter as well.

Assuming the modulation signal  $V_M$  is a sinusoidal voltage with angular frequency  $\omega_m$  and amplitude  $V_m$  superimposed on a DC voltage  $V_B$  we get:

$$V_M = V_B + V_m \sin(\omega_m t) \quad (6)$$

Using (4) we obtain:



$$\begin{aligned} \frac{I_O}{AI_I} &= \frac{1}{2} \left\{ I + \cos \left[ \frac{\pi}{V_\pi} (V_B + V_m \sin(\omega_m t)) \right] \right\} = \\ &= \frac{1}{2} \left\{ I + B \cos[C \sin(\omega_m t)] - D \sin[C \sin(\omega_m t)] \right\} \quad (7) \end{aligned}$$

where  $B = \cos(\pi V_B / V_\pi)$ ,  $C = \pi V_m / V_\pi$ ,  $D = \sin(\pi V_B / V_\pi)$  and we used the trigonometric relations:

$$\begin{aligned} \cos^2 \theta &= \frac{1}{2} (1 + \cos 2\theta) \\ \cos(a + b) &= \cos a * \cos b - \sin a * \sin b \quad (8) \end{aligned}$$

Using the relations:

$$\begin{aligned} \sin(x \sin \theta) &= 2 \sum_{n=1}^{\infty} J_{2n-1}(x) \sin[(2n-1)\theta] \\ \cos(x \sin \theta) &= J_0(x) + 2 \sum_{n=1}^{\infty} J_{2n}(x) \cos[2n\theta] \quad (9) \end{aligned}$$

where  $J_n(x)$  are the Bessel functions of the first kind, we can rewrite (7) as follows:

$$\frac{I_O}{AI_I} = \frac{1}{2} \left\{ I + B J_0(C) + 2B \sum_{n=1}^{\infty} J_{2n}(C) \cos(2n\omega_m t) - 2D \sum_{n=1}^{\infty} J_{2n-1}(C) \sin[(2n-1)\omega_m t] \right\} \quad (10)$$

A particular bias voltage point of interest is at  $V_B = V_\pi / 2$  also known as the “quadrature bias point”. At this particular bias voltage,  $B=0$ ,  $D=1$  and (10) becomes:

$$\frac{I_O}{AI_I} = \frac{1}{2} \left\{ I - 2 \sum_{n=1}^{\infty} J_{2n-1}(C) \sin[(2n-1)\omega_m t] \right\} \quad (11)$$

which means that only the fundamental frequency of the modulation signal and its odd harmonics are present. Further, if  $V_m = V_\pi / 2$  (100% modulation index) then the first three components of the series in (11) are:  $J_1=0.567$ ,  $J_3=0.069$  and  $J_5=0.0022$  which means that the 3<sup>rd</sup> harmonics amplitude is only 12.2% of the fundamental and 5<sup>th</sup> harmonics content is only 3.9% of it. For 50% modulation index, the 3<sup>rd</sup> harmonics amplitude is only 2.7% of the fundamental and 5<sup>th</sup> harmonics content is only 0.021% of it. The immediate conclusion is that although the transfer function of the modulator is nonlinear (cosine square), the harmonics content at the “quadrature bias point” is low to moderate even at very large modulation indices.

## 2.2 The dispersion parameter measurement

The technique used in this experiment is based on the analytical approach describing the behavior of SMF fibers reported by Hakki [9]. The optical signal modulated by an RF signal, using the Mach-Zehnder external modulator, is launched into the fiber. This signal is attenuated and dispersed by the fiber. The total optical power at the input and the output of the fiber (with length  $L_F$ ) is measured by a photodetector ( $I_{det}$ ) and a spectrum analyzer measures the RF signal amplitude ( $V_{RF}$ ), detected by the same detector. Then, using the relation

$$\Delta P = 20 \log \frac{V_{RF}(L_F)}{V_{RF}(0)} - 20 \log \frac{I_{det}(L_F)}{I_{det}(0)} \quad (12)$$

we eliminate the attenuation of the fiber. The quantity  $\Delta P$  will allow us to calculate the Dispersion parameter of the fiber, using the following theoretical approach.

In the following, it is assumed a symmetrical two arms Mach-Zehnder modulator with both arms biased at the "quadrature point" and modulated by two RF signals with a phase difference of  $\pi$  radians, as follows:

$$V_{M1} = \frac{V_\pi}{2} - V_{m1} \cos(k_m x); \quad V_{M2} = -\frac{V_\pi}{2} + V_{m2} \cos(k_m x) \quad (13)$$

and  $V_{m1} + V_{m2} = V_\pi$ ;  $k_m = \omega_m / v$ ,  $v = c / n_0$  is the propagation velocity ( $c$  is the speed of light in vacuum).

Inserting these expressions in (1) leads to:

$$E_O(x) = E_I \cos \left[ \frac{\pi}{4} (1 - \cos(k_m x)) \right] e^{j(k_0 x + \phi(x))}; \quad \phi(x) = -\frac{\pi}{4} \frac{1-r}{1+r} \cos(k_m x) \quad (14)$$

The normalized optical field in the forward traveling wave launched from the Mach-Zehnder modulator into the fiber is given by:

$$E_f(x) = \frac{E_O}{E_I} = e^{jk_0 x} \left[ A_0 + \sum_{N=1}^{\infty} A_N \cos(Nk_m x) \right] \quad (15)$$

where:

$$k_o = \beta / n_o = 2\pi n_o / \lambda; \quad n_o = \text{fiber refraction index} \quad (16)$$

$$A_0 = a_0 - j b_0 \quad (17)$$

$$A_N = a_N - jb_N \quad (18)$$

$$a_0 = J_0(\zeta) + J_0(\xi) \quad (19)$$

$$b_0 = J_0(\xi) - J_0(\zeta) \quad (20)$$

$$a_N = 2 \left[ \cos\left(\frac{n\pi}{2}\right) + \sin\left(\frac{n\pi}{2}\right) \right] [J_N(\zeta) + J_N(\xi)] \quad (21)$$

$$b_N = 2 \left[ \sin\left(\frac{n\pi}{2}\right) - \cos\left(\frac{n\pi}{2}\right) \right] [J_N(\zeta) - J_N(\xi)] \quad (22)$$

$J_N(z)$  being the Bessel function of the first kind and order N.

$$\zeta = \frac{\pi(1+\alpha)}{4} \quad (23)$$

$$\xi = \frac{\pi(1-\alpha)}{4} \quad (24)$$

$$\alpha = \frac{1-r}{1+r} \quad (25)$$

$$r = \frac{V_{m2}}{V_{m1}} \quad (26)$$

The parameter,  $\alpha$ , is called the ‘‘chirp parameter’’ and it can be observed that for  $\alpha=0$  ( $r=1$  or  $V_{m1}=V_{m2}$ ), the frequency chirp  $\phi$  from expression (14) above, is equal to zero. At the output of the fiber, the normalized optical field at any time  $t$ , is given by:

$$E_f(x') = \frac{1}{2} e^{jk_0 x'} \left[ A_0 + \sum_{N=1}^{\infty} A_N e^{-j\psi N^2 k_m^2} \cos(Nk_m x') \right] \quad (27)$$

where

$$x' = x - vt \quad (28)$$

$$\psi = \frac{\lambda^2 L_F D v}{4\pi n_o^2} \quad (29)$$

and  $D$  is the dispersion parameter in ps/nm.km. The power associated with this field is given by:

$$P_f(x') = \sum_{N=0}^{\infty} P_N \cos(Nk_m x') \quad (30)$$

where

$$P_0 = |A_0|^2 + \frac{1}{2} \sum_{N=1}^{\infty} |A_N|^2 \quad (31)$$

$$P_1 = \text{Re} \left\{ 2A_0 A_1^* e^{j\psi k_m^2} + \sum_{N=1}^{\infty} A_N A_{N+1}^* e^{j\psi k_m^2 (2N+1)} \right\} \quad (32)$$

$$P_2 = \frac{1}{2} |A_1|^2 + 2 \text{Re} \left[ A_0 A_2^* e^{j4\psi k_m^2} \right] + \text{Re} \sum_{N=1}^{\infty} A_N A_{N+2}^* e^{j\psi k_m^2 4(N+1)} \quad (33)$$

and the coefficients of higher order can be obtained in a similar manner. In our experiment, we are interested in the power contained in the fundamental modulating frequency signal,  $P_1$ . Therefore,  $\Delta P$  as defined in (12) can be evaluated as follows:

$$\Delta P = 20 \log \left| \frac{P_1(L_F)}{P_1(0)} \right| \quad (34)$$

Assuming all the fiber and modulator parameters (others than  $D$ ) are known, one can calculate the Dispersion parameter by measuring  $\Delta P$  at one single frequency  $f_m$  and use of relation (34). It turns out that expression (34) has a periodic behavior with zeroes (notches) at certain  $\psi k_m^2$  values [10]. Figure 2 shows a plot of  $\Delta P$  as a function of  $\psi k_m^2$ , for  $r=0$  and  $\alpha=1$ .

Experimentally, detecting the frequency of the first notch will be the most accurate measurement, since only a Spectrum analyzer is needed and the accuracy of frequency measurements with this instrument is very good. On any other point of the  $\Delta P$  graph, both frequency and attenuation need to be measured and attenuation measurements are less accurate because of power fluctuation due to laser and power meter stability and noise. In the experiment detailed in the next section, we measure the notch frequency and derive the dispersion parameter of the fiber.

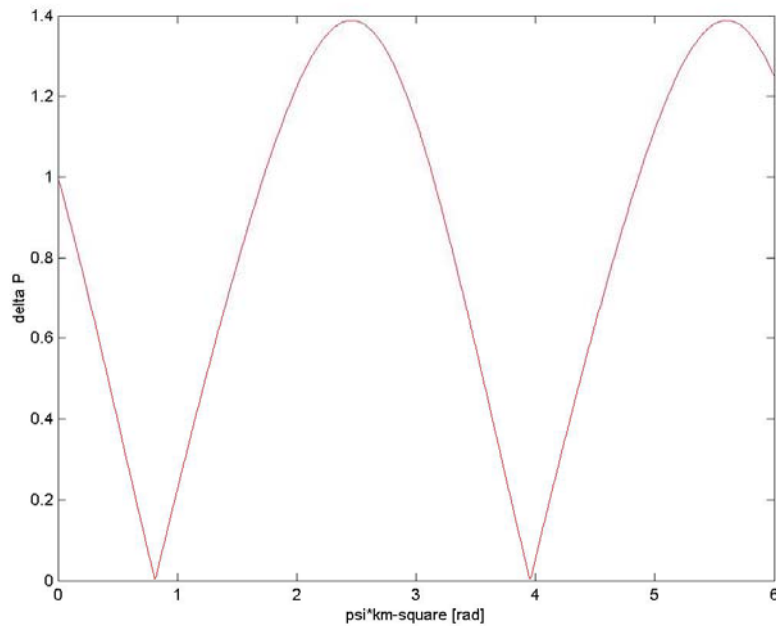


Figure 2 – Typical behavior of  $\Delta P$  as a function of  $\psi k_m^2$  for  $\alpha=1$

### 3. Experimental Setup and Results

#### 3.1 Experimental Setup

The full experimental setup is shown in Figure 3. Not all the equipment was needed in all the different phases of the measurements, as will be detailed in the following paragraphs. The different components included in this setup are:

- **Laser Diode Unit.** This unit consists of a Fujitsu FLD150F1CJ thermoelectrically cooled DFB laser operating at  $1.55\mu\text{m}$  mounted on a small PC board allowing interconnections with the Laser Diode Controller. During the experiment, the Laser was operated at 50.0 mAmp and  $22.5^\circ\text{C}$ . The output power of the laser at this operational bias point was  $\sim 1.5\text{mW}$ .
- **Laser Diode Controller.** This instrument is an ILX Lightwave Model LDC-3722 Controller allowing careful control over Laser Diode Current and Temperature. The thermistor coefficients required for accurate temperature measurement and control, have been calculated using the Laser Diode data sheet specifications, as detailed in Appendix B.
- **Mach-Zehnder Modulator.** This is a Sumitomo Cement SCC T-MZ-1.5-20 device with a  $>18\text{GHz}$  bandwidth, capable to operate at data-rates of up to  $20\text{Gbit/sec}$ .

The device is a LiNbO<sub>3</sub> Z-cut Coplanar Structure (CPS) Intensity Modulator including an embedded polarizer at the input port (see detailed Data Spec. in Appendix A). The RF+DC bias is supplied to the input electrical (SMA) connector while the output connector is loaded by a 50Ω termination.

- **Single Mode Fiber (SMF) Spool.** Two spools, 19.8km of standard SMF each (made by Corning), have been used during the experiment. All the optical interconnections are standard FC/PC connectors and adaptors.
- **RF Signal Generator.** The HP 8620A Sweep Oscillator with 4 frequency bands covering the range of 0.2-12GHz was used (for  $f_m=100\text{MHz}$ , we used a different signal generator). The maximum output power of the Generator is around +10dBm.
- **Bias Tee.** This device made by Sierra Microwave Technology, model SM41170, with a 2-18GHz bandwidth has been used to combine the DC Bias and the RF signal for the MZ Modulator.
- **Photo-Detector Head.** The AR-D25 Photo-Detector head made by Antel-Optronics has a bandwidth of DC-10GHz and responsivity of ~25 A/W into 50Ω load.

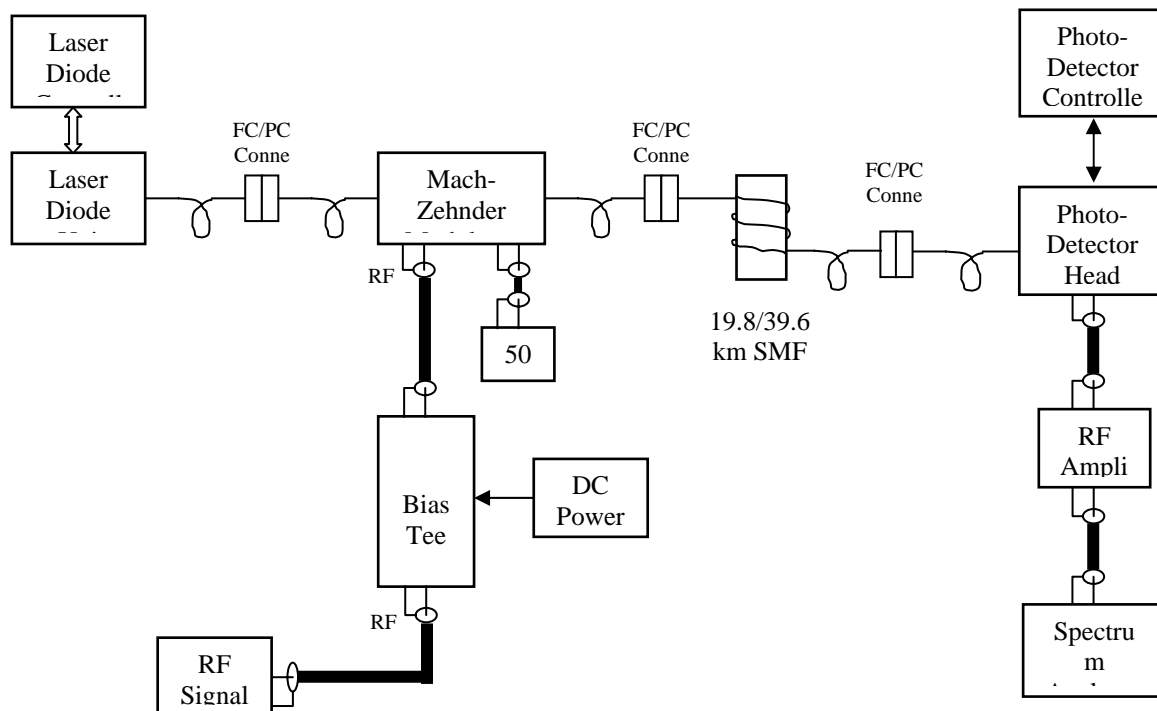


Figure 3 – Schematic diagram of the experimental setup

- **Photo-Detector Controller.** This unit, model PS-025, supplies the bias voltage to the photo-detector, measures and displays the photo-detector current, which is directly proportional to the total optical power detected by the photo-detector.
- **RF Amplifier.** This amplifier (by Planar Electronics), model PE2-20-0R38-15-SFF, with 0.1-12GHz (-3dB bandwidth) and 20dB Gain is used in measurements where the Photo-Detector signal is close to the noise level of the Spectrum Analyzer.
- **Spectrum Analyzer.** The HP Spectrum Analyzer, with a 9kHz-22GHz bandwidth, has been used to measure the RF signal amplitudes at the input of the MZ Modulator and at the output of the Photo-Detector Head.

### 3.2 Measurement of the Mach-Zehnder Modulator Transfer Function

As a first step, it is necessary to measure the modulator transfer function, the optical output power as a function of DC Bias). This measurement allows us to define the main parameters of the modulator as: insertion loss,  $V_{\pi}$  and extinction ratio.

The setup used for this measurement is actually a sub-setup of full setup described above and shown in Figure 3. All the RF equipment was unnecessary as well as the SSMF spools.

The Modulator was supplied with a variable DC voltage provided by the variable Laboratory DC Power Supply. The Photo-Detector was connected to the optical output of the Modulator and its current was recorded. Some of the results are listed in **Table 1**, below and full graphs of the Modulator Transfer Curve as well as the  $\cos^2$  approximation are shown in **Figure 4**.

Measured Parameter	Value
MZ Input Optical Power (Idet)	(1110±2)μA
MZ Maximum Output Power (Idet)	(267±3)μA
MZ Minimum Output Power (Idet)	(1.8±0.1)μA
DC Bias, $V_{BMAX}$ @ Max. Out Power	-3.35V
DC Bias, $V_{BMIN}$ @ Min. Out Power	+1.1V

Table 1 – Measured parameters

Using the listed above parameters we can determine:

$$\text{Insertion Loss (IL)} = 10 \log \frac{267}{1110} = 6.19 \text{ dB}$$

$$V_{\pi} = V_{BMIN} - V_{BMAX} = 1.84 + 3.1 = 4.45 \text{ V}$$

$$\text{Extinction Ratio} = 10 \log \frac{267}{1.8} = 21.7 \text{ dB}$$

The same measured parameters in Data Specification of this Modulator (as measured by the manufacturer) are: I.L.=3.7dB,  $V_{\pi}$ =4.8V Extinction Ratio=28dB. As we can see some degradations occurred in both the I.L and Extinction Ratio parameters. Also, the transmission function of the Modulator is shifted, so the maximum transmission is achieved at -3.35V, instead of 0V. Therefore, this function can be approximated by (4), with an additional constant phase shift  $\Phi$ , as follows:

$$\frac{I_O}{AI_I} = \cos^2 \left( \frac{\pi V_M}{2V_{\pi}} + \Phi \right) = \cos^2 \left( \frac{\pi V_M}{8.9} + 1.24 \right) \quad (35)$$



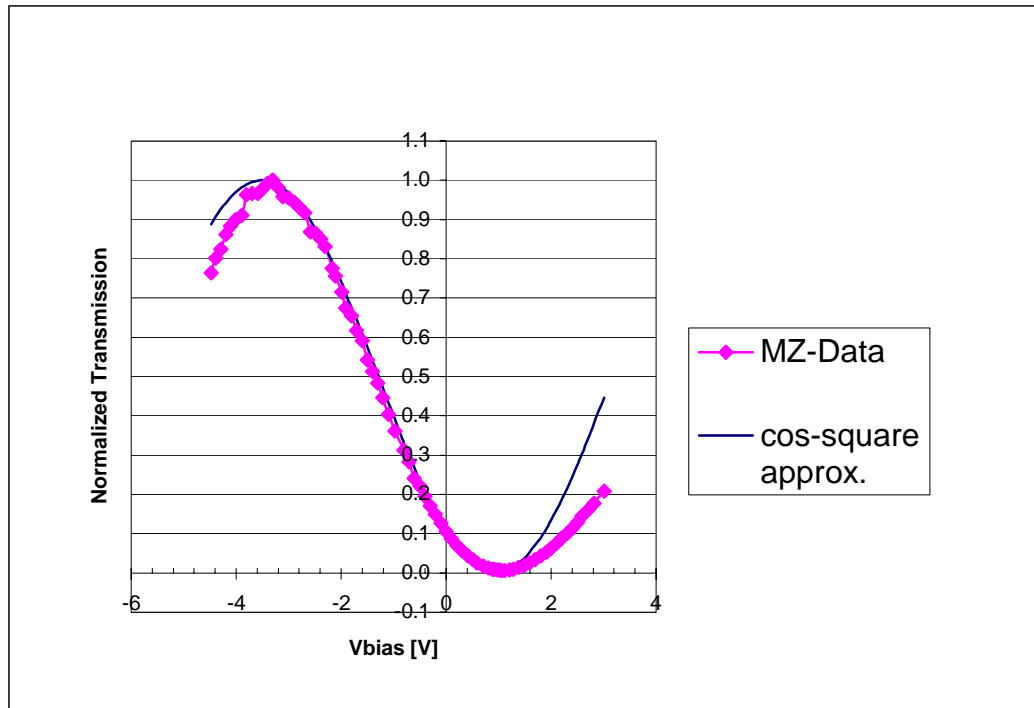


Figure 4 Measured transmission function and theoretical  $\cos^2$  fit

As we can see the theoretical curve given in (35) gives a very good approximation for the measured transmission function of the modulator, within the operating region of  $V_{BMAX} < V_M < V_{BMIN}$ .

### 3.3 Measurement of Dispersion Parameter

These measurements were done in two steps: first, we used the experimental setup shown in Figure 3, with one spool of SM fiber of 19.8 km.

The Mach Zehnder Modulator was biased at the quadrature point,  $V_B = -1.35V$  resulting in  $I_{DET} = (130 \pm 2)\mu A$ . The total optical output power at the input and the output of the SM fiber spool was measured throughout the entire experiment and its optical attenuation fluctuating from  $(10 \pm 0.35)dB$  for one part of the experiment to  $(10.8 \pm 0.4)dB$  for the other part of it. These small changes in attenuation were mostly because during the experiment the fiber was connected and disconnected few times, allowing measurements of the input and output power and signal for different frequency bands of the RF signal generator.

The RF signal generator frequency was swept from 3.2 GHz to 12 GHz using two bands (3.2GHz-6.5GHz) and (8GHz-12GHz). The output power was maintained at about +6dBm ( $V_m = 0.63V$ ). The RF signal amplitude detected by the Photo-Detector

and amplified by the RF Amplifier, was measured by the Spectrum Analyzer, using its Maximum-Hold function, with and without the SM fiber spool. The two sweeps results were stored in two separate traces and the ratio  $V_{RF}(L_F)/V_{RF}(0)$  was calculated automatically (using a mathematical function of the Spectrum Analyzer) by subtracting the values in the two traces (the Spectrum Analyzer was setup to store signal amplitudes in dBm). The attenuation results were manually recorded from the Spectrum Analyzer display (there was no other way of downloading the results from the instrument). Then, taking into account the fiber attenuation,  $\Delta P$  as defined in (12) was obtained. The results are detailed in Appendix C.

The same procedure was repeated for a setup including two 19.8km spools of SM fiber connected one after the other, to form a 39.6km SM fiber length. The total optical attenuation of the two spools fluctuated from  $(20\pm 0.3)$ dB for one part of the experiment to  $(21.5\pm 0.35)$ dB for the other part of it, due to the same reasons as for one spool experiment.

In order to calculate the Dispersion parameter for the fiber used in this experiment, we need to plot the fiber behavior function,  $\Delta P$  and match it with the experimental results. In our experiment a single traveling wave electrode Mach-Zehnder modulator is used. To ease the algebra and without altering the end results, we can assume a non phase shifted modulator as one described by the relation (4) above. Following the theoretical approach described in Section 3.2, we get:

$$\Delta\beta L = \beta L = \frac{\pi}{4} \left[ 1 - \frac{2V_m}{V_\pi} \cos(k_m x) \right] \quad (36)$$

and the optical field at the output of the modulator is:

$$E_O(x) = E_I \cos \left[ \frac{\pi}{4} \left( 1 - \frac{2V_m}{V_\pi} \cos(k_m x) \right) \right] e^{j(k_0 x + \phi(x))}; \quad \phi(x) = \frac{\pi}{4} \left( 1 - \frac{2V_m}{V_\pi} \cos(k_m x) \right) \quad (37)$$

where

$$V_{m1} = V_m = 0.63V; \quad V_{m2} = 0; \quad r = \frac{V_{m2}}{V_{m1}} = 0; \quad \alpha = \frac{1-r}{1+r} = 1;$$

$$\zeta = \frac{\pi V_m}{V_\pi} = 0.4448; \quad \xi = 0$$

Since  $J_0(0.4448)=0.9511$  and  $J_4(0.4448)=1*10^{-4}$ , in the calculation of  $P_1$  as given by (32), we can neglect terms including the Bessel functions of order 4 and higher. We have calculated results using (35), for the above parameters and  $\lambda=1.55\mu\text{m}$  and  $n_0=1.47$ . After few iterations, we found that the best match for both  $L_F=19.8\text{km}$  and  $L_F=39.6\text{km}$  is obtained at  $D=20.6\text{ps}/\text{nm}\cdot\text{km}$ . The calculations are shown in **Figure 5** and 7 below, compared with the measured results.

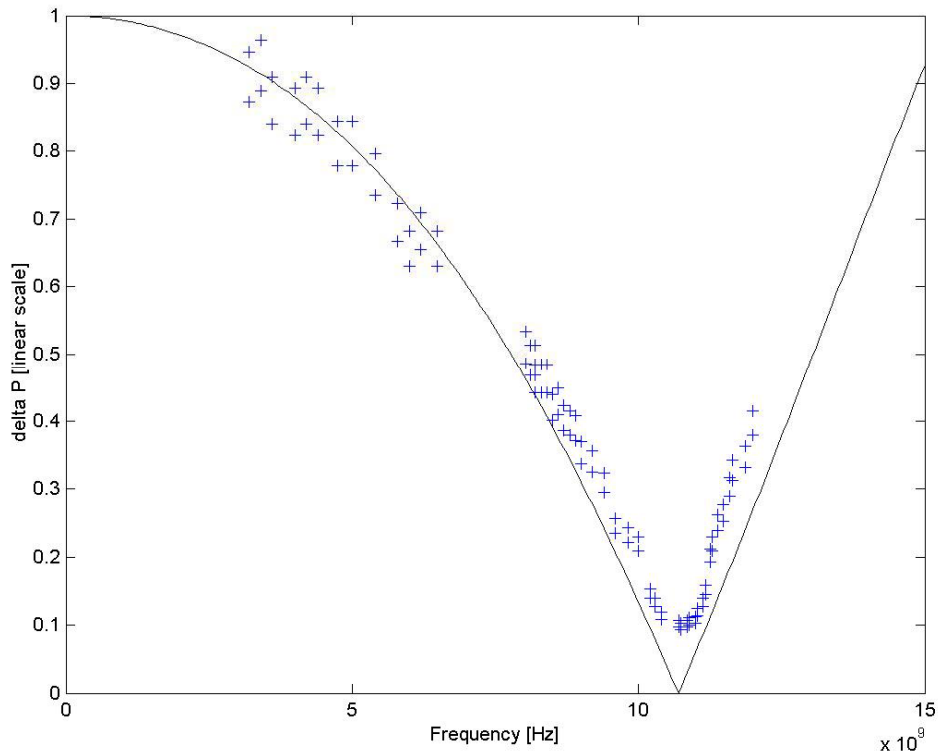


*Figure 5 – Experimental results (error bars) and calculated results for fiber spool length  $L_F=19.8\text{km}$*

The calculated results for  $D=20.6\text{ps}/(\text{nm}\cdot\text{km})$  and  $L_F=19.8\text{km}$  (see **Figure 5**) show a notch ( $\Delta P=0$ ) at  $f_m=(10.75\pm 0.025)\text{GHz}$  (the  $f_m$  steps in calculation have been chosen at  $0.05\text{GHz}$ ). There is a good agreement between the calculations and the experimental results and the minimum  $\Delta P$  is measured at  $(10.78\pm 0.067)\text{GHz}$  (see measurement results in Appendix C).

The calculated results for  $D=20.6\text{ps}/(\text{nm}\cdot\text{km})$  and  $L_F=39.6\text{km}$  (see **Figure 6**) show a notch ( $\Delta P=0$ ) at  $f_m=(7.55\pm 0.025)\text{GHz}$ . There is a good agreement between the calculations and the experimental results but, unfortunately, the notch could not be detected in the experiment, since the RF Generator we used did not cover the

frequency band of 6.5GHz-8GHz. An approximate value for this frequency can be predicted assuming a linear dependence of this value with  $\psi k_m^2$ .

Using this approximation,  $f_{m\text{-notch}@39.8km} = f_{m\text{-notch}@19.8km} * \sqrt{(19.8/39.6)} = 7.623\text{GHz}$ .

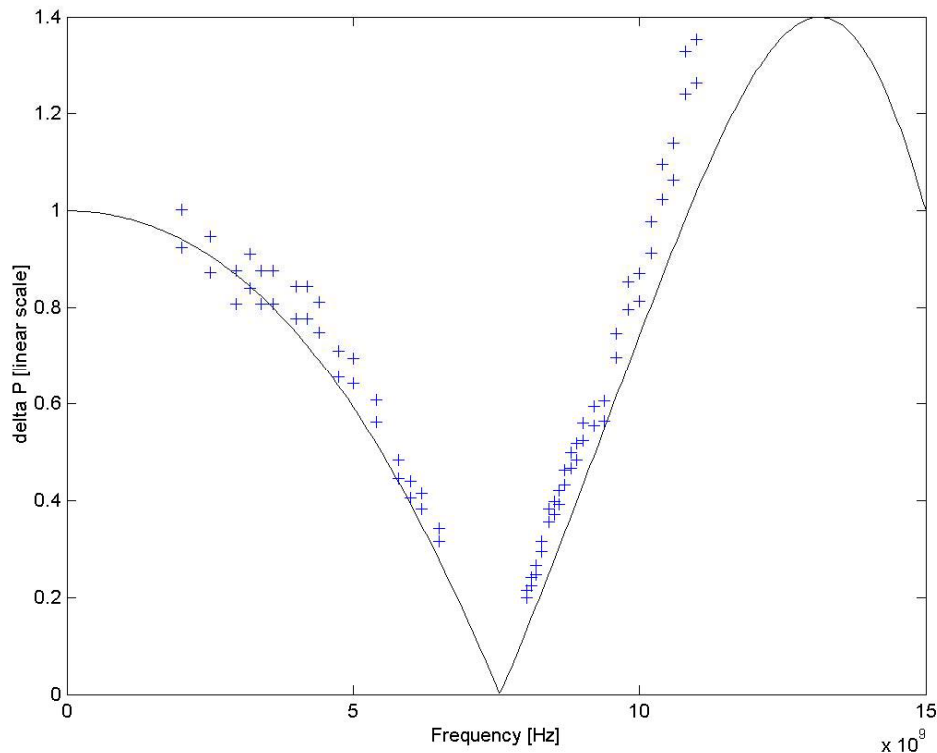


Figure 6 – Experimental results (error bars) and calculated results for fiber spool length  $L_F=39.6\text{km}$

In conclusion, this setup allows measuring with good accuracy (less than 1%) the frequency of the notch in  $\Delta P$  and with some quite simple calculation the Dispersion parameter of the fiber can be found. Moreover, for a fixed fiber length, one can calculate the notch frequency for few Dispersion parameter values and draw a graph. Then the measured notch frequency can be placed on the graph and find immediately the corresponding Dispersion parameter value.

## REFERENCES

- [1] Farbert, G. Mohs, S. Spalter, J. P. Elbers, A. Schopflin, E. Gottwald, C. Scheerer and C. Glingener, "7 Tbits/s (176X40 Gbit/s) bi-directional interleaved transmission with 50Ghz channel spacing", in Proc. ECOC, Munchen, Germany, 2000, PD 1.3, pp. 1-2.

- [2] G. P. Agrawal, "Fiber-Optic Communication Systems", ch. 3.3.7, J. Wiley & Sons, Sec. Ed. ISBN 0-471-17540-4, 1997.
- [3] R. C. Alferness, "Waveguide Electrooptic Modulators", IEEE Trans. Microwave Theory Tech., Vol. MTT-30, No. 8, Aug. 1982.
- [4] E. L. Wooten & al. "A review of Lithium Niobate Modulators for Fiber-Optic Communications Systems", IEEE J. Selected Topics in Quantum Elect., Vol. 6, No. 1, Jan/Feb 2000, pp. 69-81.
- [5] F. Koyama and K. Iga, "Frequency chirping in external modulators", J. Lightwave Technology, Vol. 6, No. 1, Jan. 1988, pp. 87-93.
- [6] K. Kawano, T. Kitoh, H. Jumoni, T. Nozawa and M. Yanagibashi, "New Traveling-Wave Electrode Mach-Zehnder Optical modulator with 20GHz Bandwidth and 4.7V driving voltage at 1.52 $\mu$ m Wavelength", Electron. Lett. Vol. 25, No. 20, Sept. 1989, pp. 1382-1383.
- [7] R. A. Becker, "Broad-Band Guided-Wave Electrooptic Modulators", IEEE J. Quantum Elect., Vol. 20, No.7, July 1984.
- [8] H. Cox, G. E. Betts and L. M. Johnson, "An Analytic and Experimental Comparison of Direct and External Modulation in Analog Fiber-Optic Links", IEEE Trans. Microwave Theory Tech., Vol. MTT-38, No. 5, May 1990.
- [9] W. Hakki, "Dispersion of Microwave-Modulated Optical Signals", IEEE J. Lightwave Technology, Vol. 11, No. 3, March 1993, pp. 474-480.
- [10]** G.H. Smith, D. Novak and Z. Ahmed, "Technique for Optical SSB Generation to overcome Dispersion penalties in Fibre-Radio systems", Electronics Letters, Vol. 33 No. 1, Jan. 1997.

### Appendix B. – Thermistor’s Coefficients calculation for Fujitsu FLD150F1CJ Laser

The ILX Lightwave Model LDC-3722 Controller used in the experimental setup, monitors and controls the laser’s temperature, using the Steinhart-Hart equation. This equation (approximated for C=0) gives the relation between the thermistor’s resistance and the ambient temperature, in the following form:

$$\frac{1}{T} = A + D \ln R(T) \quad (A1)$$

where: T- ambient (measured) absolute temperature [°K] ; R(T) - Thermistor’s resistance at temperature T ; A, D –Coefficients of the specific thermistor.

The Fujitsu catalog defines the laser’s thermistor in a different way, as follows:

$$R(T) = R_{TR} \exp \left[ B \left( \frac{1}{T} - \frac{1}{T_0} \right) \right] \quad (A2)$$

where: T- ambient (measured) absolute temperature [°K] ; T<sub>0</sub> – (273+25)=298°K; R<sub>TR</sub> – R(T<sub>0</sub>), given in the catalog, 10kΩ; B – constant, given in the catalog, 3900.

After some algebraic manipulations, (A2) can be rewritten in the following form:

$$\frac{1}{T} = \frac{1}{T_0} - \frac{1}{B} \ln(R_{TR}) + \frac{1}{B} \ln R(T) \quad (A3)$$

In (A3) one can identify the two constants of the Steinhart-Hart equation given in (A1), as follows:

$$A = \frac{1}{T_0} - \frac{1}{B} \ln(R_{TR}); \quad D = \frac{1}{B}$$

Using the constants from the catalog, we get: A=9.94\*10<sup>-4</sup> and B=2.56\*10<sup>-4</sup>.

**Appendix C: Measurement results for one SM fiber spool (19.8km) and two fiber spools (39.6km)**

<b>f [GHz]</b>	<b><math>20\log[V_{RF}(L_F)/V_{RF}(0)]</math></b>	<b><math>\Delta P</math> [dB]</b>
0.1	-(9.0±0.4)	+(0.4±0.6)
0.2	-(9.3±0.4)	+(0.1±0.6)
0.5	-(9.7±0.4)	-(0.3±0.6)
1.0	-(9.8±0.4)	-(0.4±0.6)
1.5	-(10.0±0.6)	-(0.6±0.8)
2.0	-(9.4±0.3)	(0.0±0.5)
3.0	-(8.9±0.4)	+(0.5±0.6)
4.0	-(8.9±0.4)	+(0.5±0.6)
5.0	-(9.0±0.4)	+(0.4±0.6)
6.0	-(7.6±0.3)	+(1.8±0.5)
6.5	-(6.7±0.5)	+(2.7±0.7)
8.0	-(6.8±0.5)	+(2.6±0.7)
9.0	-(6.3±0.4)	+(3.1±0.6)
10.0	-(5.2±0.8)	+(4.2±1.0)
11.0	-(4.7±1.3)	+(4.7±1.5)

**Table 2.** – *Experimental results with one 19.8km SM fiber spool*